

Higgs boson pair production and decay at NLO in QCD: the $b\bar{b}\gamma\gamma$ final state

Hai Tao Li,^a Zong-Guo Si,^a Jian Wang,^{a,b} Xiao Zhang,^a Dan Zhao^a

^a*School of Physics, Shandong University, Jinan, Shandong 250100, China*

^b*Center for High Energy Physics, Peking University, Beijing 100871, China*

E-mail: haitao.li@sdu.edu.cn, zgsi@sdu.edu.cn, j.wang@sdu.edu.cn,
zhaangx@mail.sdu.edu.cn, zhaodan@mail.sdu.edu.cn

ABSTRACT: The Higgs boson pair production at the LHC provides a probe to the Higgs boson self-coupling. The higher-order QCD corrections in this process are sizable and must be taken into account in comparison with data. Due to the small cross section, it is necessary to consider at least one of the Higgs bosons decaying to bottom quarks. The QCD corrections to the decay processes would also be important in such cases. We present a full calculation of the total and differential cross sections for the $b\bar{b}\gamma\gamma$ final state with next-to-leading order (NLO) QCD corrections. After applying typical kinematic cuts in the final state, we find that QCD NLO corrections in the decay decrease the LO result by 19% and reduce the scale uncertainties by a factor of two. The QCD corrections to the invariant mass $m_{jj\gamma\gamma}$ distribution, the transverse momentum spectra of the leading bottom quark jet and photon are significant and can not be approximated by a constant factor.

Contents

1	Introduction	1
2	Calculation framework	2
3	Numerical results	4
4	Conclusion	8
A	$H \rightarrow b\bar{b}$ decay	11
B	$H \rightarrow \gamma\gamma$ decay	12

1 Introduction

The discovery of the Higgs boson more than ten years ago [1, 2] marks the great success of the standard model (SM), and inaugurates a new era in particle physics. The presence of a Higgs field is essential to explain the masses of the W and Z gauge bosons via the Higgs mechanism [3–6]. Until now, the properties of this Higgs boson, including its mass and width [7–9], spin and parity [10, 11], as well as various production and decay rates [12, 13], have been measured, and the results are in agreement with the SM predictions.

A precise understanding of the trilinear Higgs self-coupling λ_{HHH} is crucial for unraveling the mechanism of electroweak symmetry breaking and offering insights into vacuum stability [14]. The self-interaction of the Higgs boson contributes to higher-order electroweak corrections in both the production and decay processes of a single Higgs boson, and thus the Higgs self-coupling gets constrained by precisely measuring the cross sections of the single Higgs processes [15–20]. However, this method relies on the assumption that there is no modification of the other Higgs couplings [21], and the dependence appears as a loop effect. Therefore, it is more informative to measure the Higgs boson pair productions, which are sensitive to the trilinear Higgs self-coupling at leading order (LO).

At the LHC, the gluon fusion is the dominant production channel, in which the Higgs bosons are emitted from a top quark loop. The cross section of this process has been calculated up to QCD N³LO in the infinite large top quark mass limit [22–26] and up to QCD NLO with finite m_t dependence [27–30]. In the $m_t \rightarrow \infty$ limit, the NLO corrections are significant, increasing the LO results by 87%, and the NNLO corrections provide an additional 33% enhancement. The N³LO corrections amount to about 6.4% of the LO cross sections. With finite top quark mass, the NLO QCD corrections increase the LO cross section by 66%. Partial m_t effects at NNLO in QCD and the electroweak corrections at NLO have been studied in [31–34] and [35–39], respectively. Soft gluon resummation effects have been taken into account in [40–42].

The CMS collaboration has searched for the Higgs pair productions in the $b\bar{b}\gamma\gamma$, $b\bar{b}b\bar{b}$, $b\bar{b}\tau\tau$, $b\bar{b}ZZ$ and multilepton final states, giving a limit of 3.4 times the cross section predicted by the SM at 95% confidence level (CL), which is converted to the allowed range for the self-coupling $-1.24 < \kappa_\lambda (= \lambda_{HHH}/\lambda_{HHH}^{\text{SM}}) < 6.49$ at 95% CL [13]. The ATLAS collaboration has measured the Higgs pair productions in the $b\bar{b}\gamma\gamma$, $b\bar{b}\tau\tau$, and $b\bar{b}b\bar{b}$ final states, and set an upper limit of 2.4 times SM predictions. Combined with the single Higgs boson analyses, this is transformed to the constraint $-0.4 < \kappa_\lambda < 6.3$ at 95% CL [19]. The range would be significantly narrowed at the high-luminosity LHC [43].

In obtaining the above limits, precise predictions for the kinematic distributions of the HH events, especially the m_{HH} distribution, play an important role [44]. So far, only the higher-order QCD corrections in the production processes have been studied. It is not clear whether the kinematic distributions would change after considering the QCD corrections in the decays of the Higgs bosons. Our aim in this paper is to address this issue. Because the cross section of the Higgs boson pair production is already very small, it is required to search for the signal events with at least one of the Higgs bosons decaying to two bottom quarks. We focus on the $HH \rightarrow b\bar{b}\gamma\gamma$ final state in the present work. We find that the NLO QCD correction in the decay could reduce the cross section for the process $pp \rightarrow HH \rightarrow b\bar{b}\gamma\gamma$ significantly and that the impact on the kinematic distributions can not be described by a constant.

This paper is organized as follows. In section 2, we introduce the calculation framework. The numerical results for the total cross sections and kinematical distributions are presented in section 3. The conclusion is given in section 4.

2 Calculation framework

We are going to calculate the full QCD corrections to $gg \rightarrow HH$ production with the $HH \rightarrow b\bar{b}\gamma\gamma$ decay at the LHC. The interference between the QCD corrections in the production and decay processes starts from NNLO and is suppressed by a factor of $\Gamma_H/m_H \sim 10^{-5}$ compared to the resonance contribution, in which the Higgs bosons are taken to be on-shell. In this paper, we consider only the $\mathcal{O}(\alpha_s)$ correction and therefore neglect the interference.

In the narrow-width approximation, the cross section is written as

$$\sigma_{\text{pro+dec}} = \sigma_{\text{pro}} \frac{1}{\Gamma_{H_1}} \frac{1}{\Gamma_{H_2}} \Gamma_{\text{dec}} \quad (2.1)$$

where σ_{pro} denotes the production cross section of $gg \rightarrow H_1 H_2$ and $\Gamma_{H_1} = \Gamma_{H_2} = \Gamma_H$ is the total width of the Higgs boson. The double decay width is defined by

$$\Gamma_{\text{dec}} \equiv \int d\Gamma_{H_1} \int d\Gamma_{H_2} F_J \quad (2.2)$$

with F_J the measurement function which embodies the cut information in event selection. For a specific decay mode, i.e., $H_1 \rightarrow X_1$ and $H_2 \rightarrow X_2$, the cross section is expressed as

$$\sigma_{\text{pro+dec}(X_1, X_2)} = \sigma_{\text{pro}} \frac{1}{\Gamma_{H_1 \rightarrow X_1}} \frac{1}{\Gamma_{H_2 \rightarrow X_2}} \Gamma_{\text{dec}(X_1, X_2)} \times R(H_1 \rightarrow X_1) R(H_2 \rightarrow X_2) \quad (2.3)$$

where we have introduced $R(H_i \rightarrow X_i)$ as the branching ratio for the Higgs decay into the final state X_i .

We focus on the higher-order QCD corrections to the production and decay to a specific final state $X_1 + X_2$. The cross sections and decay widths can be expanded in a series of the strong coupling constant α_s , e.g.,

$$\sigma = \sigma^{(0)} + \sum_{n=1} \alpha_s^n \sigma^{(n)}. \quad (2.4)$$

And therefore, we have

$$\begin{aligned} \sigma_{\text{pro+dec}(X_1, X_2)}^{(n)} &= \sigma_{\text{pro}} \frac{1}{\Gamma_{H_1 \rightarrow X_1}} \frac{1}{\Gamma_{H_2 \rightarrow X_2}} \Gamma_{\text{dec}(X_1, X_2)} \Big|_{\text{expanded to } \alpha_s^n} \\ &\times R(H_1 \rightarrow X_1) R(H_2 \rightarrow X_2). \end{aligned} \quad (2.5)$$

We have taken the branching ratios as constants in our calculation, and the most precise values given in refs. [45–47] are adopted.

As a first step, we incorporate only the NLO QCD corrections in this study. The $\mathcal{O}(\alpha_s)$ correction is decomposed into two parts,

$$\sigma_{\text{pro+dec}(b\bar{b}, \gamma\gamma)}^{(1)} = \sigma_{\text{pro+dec}(b\bar{b}, \gamma\gamma)}^{\text{pro}(1)} + \sigma_{\text{pro+dec}(b\bar{b}, \gamma\gamma)}^{\text{dec}(1)} \quad (2.6)$$

with

$$\sigma_{\text{pro+dec}(b\bar{b}, \gamma\gamma)}^{\text{pro}(1)} = \sigma_{\text{pro}}^{(1)} \frac{1}{\Gamma_{H_1 \rightarrow b\bar{b}}^{(0)}} \frac{1}{\Gamma_{H_2 \rightarrow \gamma\gamma}^{(0)}} \Gamma_{\text{dec}(b\bar{b}, \gamma\gamma)}^{(0)} \times R(H_1 \rightarrow b\bar{b}) R(H_2 \rightarrow \gamma\gamma) \quad (2.7)$$

and

$$\begin{aligned} \sigma_{\text{pro+dec}(b\bar{b}, \gamma\gamma)}^{\text{dec}(1)} &= \sigma_{\text{pro}}^{(0)} \frac{1}{\Gamma_{H_1 \rightarrow b\bar{b}}^{(0)}} \frac{1}{\Gamma_{H_2 \rightarrow \gamma\gamma}^{(0)}} \Gamma_{\text{dec}(b\bar{b}, \gamma\gamma)}^{(1)} \times R(H_1 \rightarrow b\bar{b}) R(H_2 \rightarrow \gamma\gamma) \\ &- \sigma_{\text{pro}}^{(0)} \frac{\Gamma_{H_1 \rightarrow b\bar{b}}^{(1)}}{\left(\Gamma_{H_1 \rightarrow b\bar{b}}^{(0)}\right)^2} \frac{1}{\Gamma_{H_2 \rightarrow \gamma\gamma}^{(0)}} \Gamma_{\text{dec}(b\bar{b}, \gamma\gamma)}^{(0)} \times R(H_1 \rightarrow b\bar{b}) R(H_2 \rightarrow \gamma\gamma) \\ &- \sigma_{\text{pro}}^{(0)} \frac{1}{\Gamma_{H_1 \rightarrow b\bar{b}}^{(0)}} \frac{\Gamma_{H_2 \rightarrow \gamma\gamma}^{(1)}}{\left(\Gamma_{H_2 \rightarrow \gamma\gamma}^{(0)}\right)^2} \Gamma_{\text{dec}(b\bar{b}, \gamma\gamma)}^{(0)} \times R(H_1 \rightarrow b\bar{b}) R(H_2 \rightarrow \gamma\gamma). \end{aligned} \quad (2.8)$$

If no cuts are applied and the full phase space of the final state particles is integrated over, $\sigma_{\text{pro+dec}(b\bar{b}, \gamma\gamma)}^{\text{dec}(1)}$ is vanishing. In practice, kinematic cuts have to be imposed to select the events. In this case, $\sigma_{\text{pro+dec}(b\bar{b}, \gamma\gamma)}^{\text{dec}(1)}$ may provide a significant correction. It is our purpose to investigate the contribution of this part.

Because there is no real correction from $H \rightarrow \gamma\gamma + g$ at NLO in QCD due to color conservation, the decay $H \rightarrow \gamma\gamma$ receives only virtual corrections. Then the third line in eq.(2.8) could cancel with part of the first line that is given by

$$\int d\Gamma_{H_1 \rightarrow b\bar{b}}^{(0)} \times \int d\Gamma_{H_2 \rightarrow \gamma\gamma}^{(1)} \quad (2.9)$$

since they have the same kinematics. As a consequence,

$$\begin{aligned} \sigma_{\text{pro+dec}(b\bar{b},\gamma\gamma)}^{\text{dec}(1)} &= \sigma_{\text{pro}}^{(0)} \frac{1}{\Gamma_{H_1 \rightarrow b\bar{b}}^{(0)}} \frac{1}{\Gamma_{H_2 \rightarrow \gamma\gamma}^{(0)}} \Gamma_{\text{dec}(b\bar{b},\gamma\gamma)}^{(0)} \left(\frac{\int d\Gamma_{H_1 \rightarrow b\bar{b}}^{(1)} F_J}{\int d\Gamma_{H_1 \rightarrow b\bar{b}}^{(0)} F_J} - \frac{\Gamma_{H_1 \rightarrow b\bar{b}}^{(1)}}{\Gamma_{H_1 \rightarrow b\bar{b}}^{(0)}} \right) \\ &\quad \times R(H_1 \rightarrow b\bar{b}) R(H_2 \rightarrow \gamma\gamma). \end{aligned} \quad (2.10)$$

We have written the first term in the bracket in differential form because it is subject to the kinematic cuts.

The above eqs.(2.6,2.7,2.10) represent the master formulae of our calculation. The $\mathcal{O}(\alpha_s)$ correction to the production process $\sigma_{\text{pro}}^{(1)}$ has been computed in [28] with full top quark mass dependence. We have checked the results independently using our code, although the two-loop $gg \rightarrow HH$ amplitude is calculated via the grid implemented in POWHEG BOX [48]. The one-loop $gg \rightarrow HHg$ and other similar $2 \rightarrow 3$ partonic amplitudes are generated by the automatic tool OpenLoops [49, 50] with the scalar integrals evaluated by Collier/OneLoop [51, 52]. All the tree-level and one-loop amplitudes of the decay process $H \rightarrow b\bar{b} + X$ are calculated employing the FeynArts [53, 54] and FeynCalc [55–57] packages. The analytical results are collected in Appendix A. The final-state bottom quarks have been taken to be massless while the Yukawa coupling of the bottom quark is kept finite. The result of the squared amplitude for the decay $H \rightarrow \gamma\gamma$ is recorded in Appendix B. The infrared divergences in the virtual and real corrections are subtracted using the dipole method [58, 59]. In constructing the analytical subtraction terms, we need the one-loop amplitude of $gg \rightarrow HH$ which is evaluated with the aid of QCDLoop [60].

3 Numerical results

In numerical calculation, the SM input parameters are set to be

$$\begin{aligned} G_F &= 1.1663787 \times 10^{-5} \text{ GeV}^{-2}, \quad m_W = 80.399 \text{ GeV}, \\ m_H &= 125 \text{ GeV}, \quad m_t = 173 \text{ GeV}, \quad m_b(m_b) = 4.18 \text{ GeV}, \\ R(H \rightarrow b\bar{b}) &= 0.5824, \quad R(H \rightarrow \gamma\gamma) = 2.27 \times 10^{-3}. \end{aligned} \quad (3.1)$$

We choose the parton distribution function (PDF) set PDF4LHC15_nlo_100_pdfas [61]. The strong coupling is evaluated using the function associated with this PDF set. The default values of the factorization scale μ_F and renormalization scale μ_R are set as $m_{HH}/2$. In the calculation of the real corrections to $pp \rightarrow HH$, we have applied a phase space cut $p_T^{\text{cut}} \sim 0.1 \text{ GeV}$ on the Higgs pair system to ensure numerical stability. Below this cut, the contributions from the squared amplitude and the differential subtraction terms cancel against each other and could be neglected. We have checked that the total cross sections are insensitive to this cut when it is chosen from 0.001 GeV to 1 GeV. A kinematic cut $s_{ij}^{\text{cut}} \sim 10^{-5} \text{ GeV}^2$ is applied to the final-state partons when considering the higher-order QCD corrections to $H \rightarrow b\bar{b}$ due to the same reason.

Before we show any numerical results, it is necessary to elaborate on the importance of including decay processes in the theoretical calculation. One crucial reason is that all

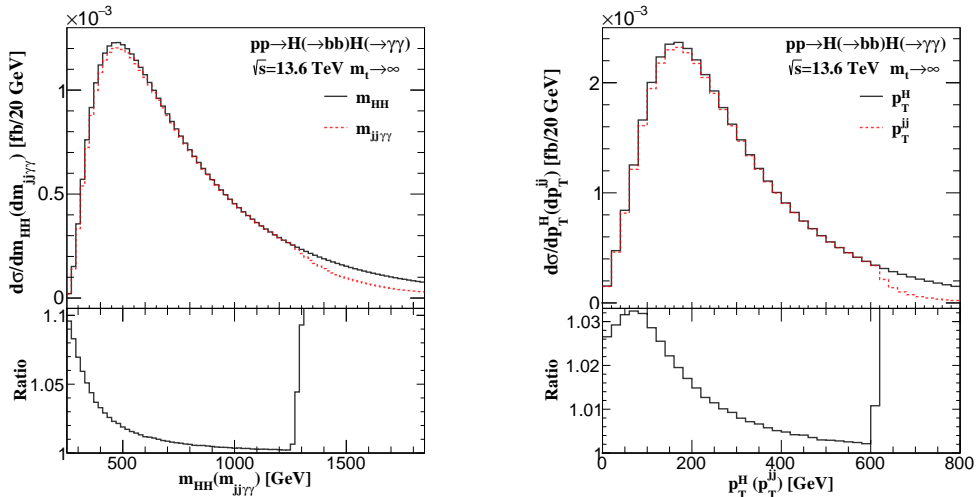


Figure 1: Comparison of the kinematic distributions for the intermediate and reconstructed Higgs bosons in the heavy top quark mass limit at LO. The lower panels show the ratio of the distributions for the intermediate Higgs bosons over those for the reconstructed Higgs bosons. The ratio rises sharply for $m_{jj\gamma\gamma}$ larger than 1200 GeV and can not be shown properly in the plot. The value is about 2.5 at $m_{jj\gamma\gamma} = 1800$ GeV. In the right plot, the ratio is about 7 at $p_T^{jj} = 800$ GeV.

the events in experiments are collected under kinematic cuts. Therefore it is the cross section with cuts that is measured. In experiments, the cuts can only be applied to the stable particles, i.e., the jets, photons, and leptons. One has to take into account the decay processes of unstable particles to fully simulate the events.

For illustration, we compare the kinematic distributions of the intermediate Higgs boson resonances and the reconstructed Higgs bosons from the final-state b -jets and photons in figure 1. The intermediate Higgs boson appears in the final state of the production process but decays to bottom quarks or photons immediately. Its momentum is known in the theoretical calculation but can not be measured directly. In contrast, the momentum of the reconstructed Higgs boson is defined as the sum of the momenta of the two b -jets, denoted by j , or the two photons. The final-state (anti-)bottom quarks and other partons are clustered to jets using the anti- k_t algorithm [62, 63] with a separation parameter $R = 0.4$. The angular distance between the photons γ and the b -jets j should be larger than 0.4. From figure 1, we see that the reconstructed invariant mass $m_{jj\gamma\gamma}$ spectrum is generally lower than the intermediate Higgs boson invariant mass m_{HH} spectrum by about 1% \sim 10% at $m_{HH}(m_{jj\gamma\gamma}) < 600$ GeV. This is mainly because the phase space with $R_{j\gamma} < R$ has been cut out. The difference becomes smaller with the increasing of $m_{HH}(m_{jj\gamma\gamma})$, because the b -jets and photons tend to fly away from each other for larger $m_{HH}(m_{jj\gamma\gamma})$. The single Higgs transverse momentum distribution is lowered by about 2% \sim 3% in the reconstructed kinematics for $p_T^{jj} < 200$ GeV, and the deviation between the distributions using the reconstructed and intermediate Higgs boson becomes smaller as $p_T^{jj}(p_T^H)$ increases from 100 GeV to 600 GeV due to the same reason in the discussion of m_{HH} .

An obvious deviation can be found in the region of $m_{HH} > 1250$ GeV or $p_T^H > 620$ GeV, where the reconstructed distribution drops quickly. The reason is that the bottom quark pair from the Higgs decay is highly boosted so that they become collinear with each other and are subject to the requirement $R_{jj} > R$. The threshold value of p_T^H can be estimated by

$$\frac{2m_H}{R} \quad (3.2)$$

which is the minimum of the momentum $p_H = m_H/R/\sqrt{z(1-z)}$ of the Higgs boson decaying to a collinear bottom (anti-)quark pair with a separation angle of R and the momentum fraction z carried by one bottom quark. One can not observe such an interesting feature without considering the decays of the Higgs bosons. Note that the distributions presented in figure 1 are obtained in the heavy top quark mass limit to show the features clearly. The distributions with finite top quark mass fall off fast. The ratios, however, exhibit similar shapes.

In practice, the particles with very low transverse momentum or very large rapidity are not detected. To calculate cross sections with decays, we apply the following cuts that are similar to those used in the analysis of the CMS collaboration [64],

$$\begin{aligned} p_T^j &\geq 25 \text{ GeV}, & p_T^\gamma &\geq 25 \text{ GeV}, & |\eta^j| &\leq 2.5, & |\eta^\gamma| &\leq 2.5, \\ 90 \text{ GeV} &\leq m_{jj} \leq 190 \text{ GeV}, & R_{jj,j\gamma,\gamma\gamma} &\geq 0.4. \end{aligned} \quad (3.3)$$

These cuts are rather loose because we want to keep more signals after cuts.

	without decays	with decays but no cuts		with decays and cuts	
		LO ^{dec}	δ NLO ^{dec}	LO ^{dec}	δ NLO ^{dec}
LO _{∞} ^{pro}	17.07 ^{+31%} _{-22%}	0.04514 ^{+31%} _{-22%}	0	0.02515 ^{+30%} _{-22%}	-0.00349 ^{+42%} _{-28%}
LO _{m_t} ^{pro}	19.85 ^{+28%} _{-20%}	0.05248 ^{+28%} _{-20%}	0	0.02789 ^{+27%} _{-20%}	-0.00523 ^{+39%} _{-27%}
δ NLO _{∞} ^{pro}	14.86 ^{+6%} _{-7%}	0.03928 ^{+6%} _{-7%}	—	0.02128 ^{+6%} _{-7%}	—
δ NLO _{m_t} ^{pro}	13.08 ^{+4%} _{-8%}	0.03458 ^{+4%} _{-8%}	—	0.01829 ^{+4%} _{-8%}	—
Full NLO result					
NLO _{∞}	31.93 ^{+18%} _{-15%}	0.08442 ^{+18%} _{-15%}		0.04294 ^{+15%} _{-14%}	
NLO _{m_t}	32.93 ^{+14%} _{-13%}	0.08706 ^{+14%} _{-13%}		0.04095 ^{+10%} _{-11%}	

Table 1: Total cross sections (in fb) of the Higgs boson pair production and decays $gg \rightarrow HH \rightarrow b\bar{b}\gamma\gamma$ at the 14 TeV LHC. The relative uncertainties are obtained by taking the seven-point scale variations around the default values. The subscripts m_t and ∞ indicate that the results are calculated with full m_t dependence or in the large m_t limit, respectively. The notation δ NLO denotes the $\mathcal{O}(\alpha_s)$ correction while the NLO results include both LO and δ NLO contributions. The symbol ‘—’ represents the higher-order corrections that we neglected in this work. The results without decays have been multiplied by 1/2 to follow the convention of identical Higgs boson pair production.

In table 1 we show the total cross sections with or without decays or cuts. The second column gives the total cross section without decays. We have performed the calculations

up to NLO in QCD both in the infinitely large m_t limit and with full m_t dependence. Our results coincide with the previous computations taken with the infinite m_t [26] and finite m_t [28] setup if the same PDF sets and SM input parameters are adopted. The LO production cross section with infinite m_t is smaller than that with finite m_t by 14%. But it receives larger QCD corrections, e.g., 87% in the infinite m_t limit compared to 66% with full m_t dependence. As a result, the difference between the two schemes is only 3% at NLO. We have estimated the scale uncertainty by varying the factorization μ_F and renormalization μ_R scales independently by a factor of two, excluding the cases when the ratio of the two scales $\mu_F/\mu_R = 4, 1/4$. We see that the scale uncertainty is reduced almost by a factor of two after including the QCD corrections.

The third column shows the total cross sections with decays but without cuts. The results with LO decays agree with the production cross sections multiplied by a product of the branching ratios, which is about 0.27%. The cross sections with the LO production and $\mathcal{O}(\alpha_s)$ decays are vanishing, as expected from eq. (2.10). These features serve as strong checks of the validity of our numerical program.

The cross sections with kinematics cuts (3.3) on the final-state jets and photons are listed in the fourth column. The results of the LO production and LO decay after the cuts are 56% and 53% of those without cuts in the infinite and finite m_t cases, respectively. The NLO corrections in the production suffer from similar suppression. The NLO corrections in the decay decrease the LO cross section by 19% (14%) for finite (infinite) m_t . This effect is much larger than the N³LO QCD correction, which is about +6% [26].

This cut rate and the NLO corrections in the decay can be understood by inspecting the transverse momentum distribution for the subleading b -jet, which is shown in figure 2. As indicated by the LO result, the transverse momentum spectrum has a peak around 40 GeV. Therefore a large portion of the events would be neglected under a typical cut $p_T^j \geq 25$ GeV on the jet. The NLO corrections can be divided into two parts, i.e., the virtual and real corrections with associated subtraction terms, denoted by $\delta\text{NLO}_{\text{V+I}}$ and $\delta\text{NLO}_{\text{R-S}}$ in the figure, respectively. The former has the same distribution as the LO because they are proportional to each other with a factor independent of the kinematics; see eq. (A.5) in the appendix. However, the latter gives a positive and negative contribution for $p_T < 30$ GeV and $p_T > 30$ GeV, respectively. The requirement of a cut $p_T^j > 25$ GeV leads to a significant cancellation between the virtual and the real corrections. As a result, the first term in the bracket in eq. (2.10) is small and the dominant contribution comes from the second term there, which is around -20%.

In figure 3, we show the influence of the QCD corrections in the decay process on some kinematic distributions. We see that the QCD corrections are most significant in the peak region of the invariant mass $m_{jj\gamma\gamma}$ distribution, which can be as large as -25%. The corrections become smaller when $m_{jj\gamma\gamma}$ moves away from the peak region. The QCD correction to the transverse momentum of the leading b -jet is also prominent in the peak region, reaching -28%. The impact of the QCD correction on the transverse momentum of the subleading b -jet is important in the small p_T region; it can reduce the LO cross section by -26%. The rapidity distribution receives a correction in the range from -21% to -18%.

In figure 4, we present the kinematic distributions including QCD NLO corrections

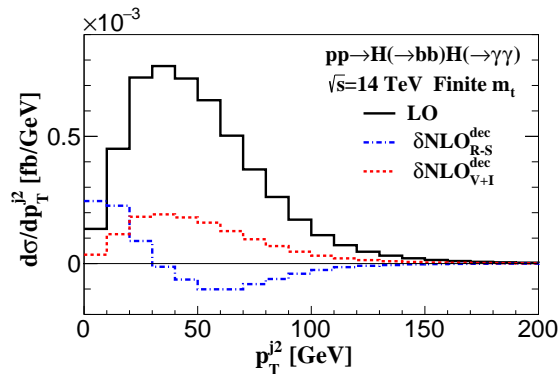


Figure 2: The transverse momentum distribution of the subleading b -jet. The black line represents the LO result. The red and blue lines denote the NLO virtual and real corrections with corresponding subtraction terms, respectively.

both in the production and the decay processes. The NLO corrections in the production increase the $m_{jj\gamma\gamma}$ distribution by 54% – 82% in the region of $m_{jj\gamma\gamma} < 600$ GeV, which contributes the dominant part of the cross section. After including the NLO corrections in the decay processes, the distribution is enhanced further for $m_{jj\gamma\gamma} < 350$ GeV but decreased for $m_{jj\gamma\gamma} > 350$ GeV. A similar pattern appears in the transverse momentum distribution of the leading b -jet. The NLO corrections in the production improve the LO results by a factor of 1.63 – 1.77, while the NLO corrections in the decay increase and decrease the cross section for $p_T^{j1} < 80$ GeV and $p_T^{j1} > 80$ GeV, respectively. The transverse momentum spectrum of the leading photon is increased by 1.62 – 1.78, considering only the QCD corrections in the production. This improvement reduces to 1.43 – 1.56 after taking the QCD corrections in the decay into account as well. The higher-order QCD corrections to the rapidity distribution of the leading b -jet are stable except for the region with very large rapidity.

4 Conclusion

The Higgs boson pair production is an important process at the LHC that can be used to measure the Higgs boson self-couplings. A precise theoretical prediction on its cross section enables an accurate and reliable constraint extracted from the present and future data. Though there has been great progress in the calculations of higher-order QCD or electroweak corrections to the production processes, the QCD corrections in the Higgs boson decays are rarely included. In this work, we present a full calculation of the QCD NLO corrections to the process $pp \rightarrow HH \rightarrow b\bar{b}\gamma\gamma$. The importance of including the decay is reflected by the difference between the kinematic distributions of the intermediate and the reconstructed Higgs bosons. After adopting loose kinematic cuts, we have found that the QCD corrections in the decay decrease the LO result by 19%. This impact is much more significant than the N^3 LO QCD corrections in the production. We also show the QCD corrections to various kinematic distributions, such as the invariant mass of the b -jets and

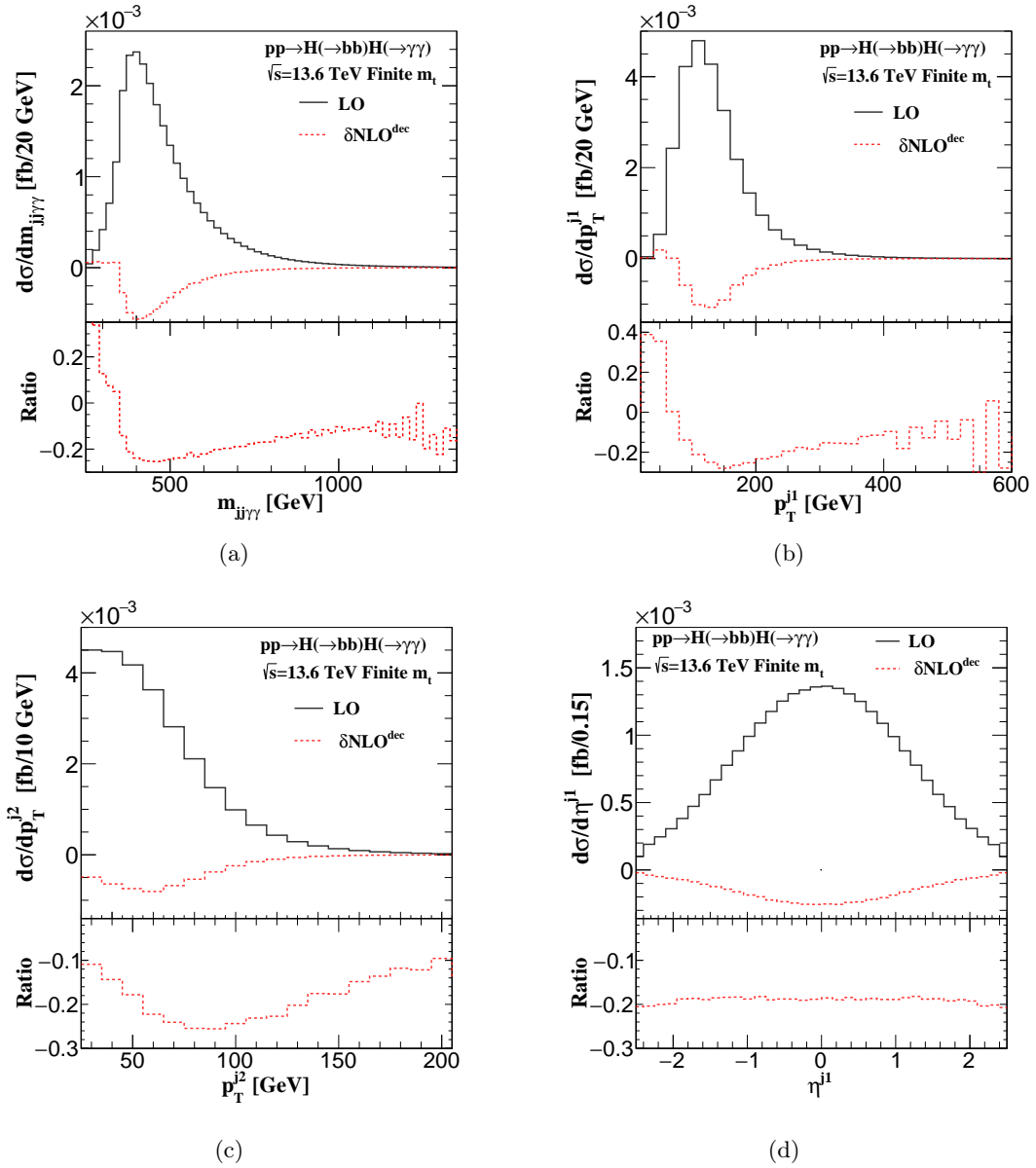


Figure 3: Impact of the QCD NLO corrections in the $H \rightarrow b\bar{b}$ decay process on the kinematic distributions after the cuts (3.3). The production cross section is calculated with finite m_t . The plot (a) shows the invariant mass of the two b -jets and two photons. The plots (b) and (c) present the transverse momenta of the leading and subleading b -jets, respectively. The rapidity distribution of the leading b -jet is shown in the plot (d). The ratio in the lower panel in each plot illustrates the magnitude of $\mathcal{O}(\alpha_s)$ corrections in the decay process compared to the LO result.

photons, the transverse momentum and rapidity distributions of the b -jets, and find that the QCD corrections in the decay process are significant, and do not change the kinematic distributions simply by a constant multiplier.

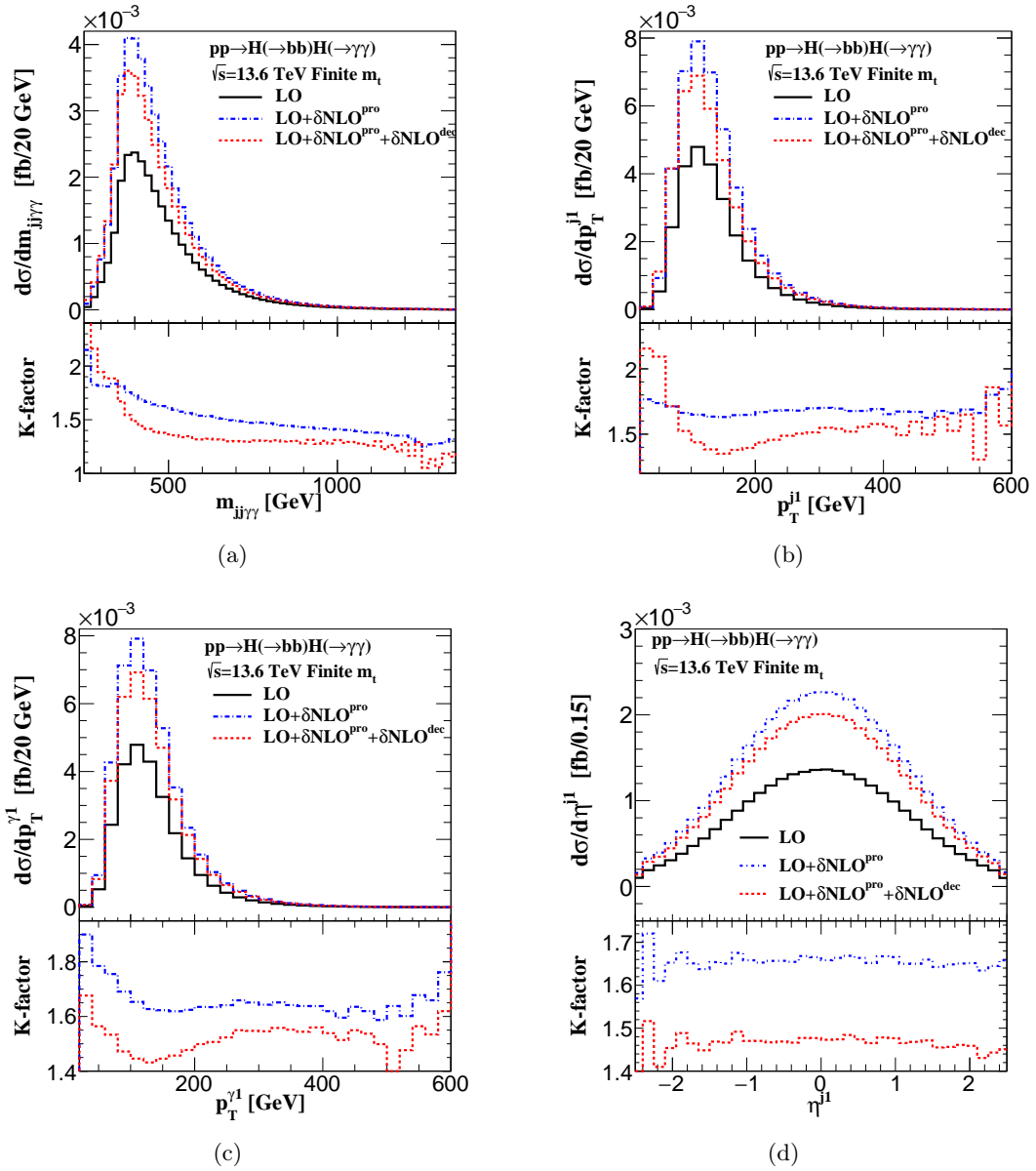


Figure 4: Kinematic distributions of the process $pp \rightarrow HH \rightarrow b\bar{b}\gamma\gamma$ after the cuts (3.3). The production cross section is calculated with finite m_t . The plot (a) shows the invariant mass of the two b -jets and two photons. The plots (b) and (c) present the transverse momenta of the leading b -jet and photon, respectively. The rapidity distribution of the leading b -jet is shown in the plot (d). The K-factor is defined as the ratio of the NLO results over the LO ones.

Acknowledgments

This work was supported in part by the National Science Foundation of China under grant Nos. 12275156, 12321005, 12375076 and the Taishan Scholar Foundation of Shandong

province (tsqn201909011).

A $H \rightarrow b\bar{b}$ decay

The Higgs boson to bottom quarks decay is the dominant channel. The QCD NLO corrections were calculated forty years ago [65–68]. The electroweak NLO corrections were obtained around the same time [69–72]. When the final-state bottom quark is taken to be massless, the inclusive and differential cross sections have been computed up to N⁴LO [73–78] and N³LO [79–81], respectively. The differential cross sections with massive bottom quarks have been calculated at NNLO in QCD [82–84], and the NNLO analytical inclusive result was studied in [85–87]. In addition, the combined QCD and electroweak corrections have been computed in [88], and the parton shower effect is considered in [89, 90].

In our calculation, we consider massless bottom quarks but keep the Yukawa coupling y_b finite. The LO squared amplitude is given by

$$|\mathcal{M}_{\text{tree}}(H \rightarrow b\bar{b})|^2 = 2\sqrt{2}N_c m_H^2 m_b^2(\mu) G_F, \quad (\text{A.1})$$

where we have replaced y_b by $2^{3/4}m_b(\mu)G_F^{1/2}$. Setting $m_H = 125$ GeV, $N_c = 3$, $m_b(m_H) = 2.8$ GeV, $G_F = 1.1663787 \times 10^{-5}$ GeV⁻² and performing phase space integration, we obtain $\Gamma_{H \rightarrow b\bar{b}}^{\text{LO}} = 1.93$ MeV. The NLO QCD corrections to $H \rightarrow b\bar{b}$ include contributions from both real and virtual gluon effects. For the real corrections, we need the tree-level amplitude squared of the process $H(p) \rightarrow b(p_1) + \bar{b}(p_2) + g(p_3)$,

$$|\mathcal{M}_{\text{real}}(H \rightarrow b\bar{b}g)|^2 = \frac{8\pi\alpha_s C_F (s_{12}^2 + m_H^4)}{s_{13}s_{23}m_H^2} |\mathcal{M}_{\text{tree}}|^2 \quad (\text{A.2})$$

with $s_{ij} \equiv (p_i + p_j)^2$. In the soft or collinear limit of the gluon’s momentum, i.e., $s_{13} \rightarrow 0$ or $s_{23} \rightarrow 0$, the integration of this amplitude squared becomes divergent. In numerical calculation, we subtract these divergences using dipole counter-terms which have the same infrared structure but are easy to integrate analytically.

The virtual loop corrections in this process are easy to compute, and the results contain both ultraviolet and infrared divergences, which are regularized by working in d -dimensional space-time with $d = 4 - 2\epsilon$. Adopting the $\overline{\text{MS}}$ and on-shell schemes for the Yukawa coupling and the bottom quark wave function, respectively, the contribution from the counter-terms is given by

$$\mathcal{M}_{\text{CT}} = -\frac{3\alpha_s C_F}{4\pi\epsilon} \mathcal{M}_{\text{tree}}, \quad (\text{A.3})$$

which would cancel the ultraviolet divergences in the loop corrections. The sum of the loop corrections and counter-terms is

$$\begin{aligned} & 2\text{Re}[\mathcal{M}_{\text{loop+CT}} \cdot \mathcal{M}_{\text{tree}}^*] \\ &= \frac{\alpha_s C_F}{2\pi} \frac{e^{\gamma_E \epsilon}}{\Gamma(1-\epsilon)} \left[-\frac{2}{\epsilon^2} - \frac{1}{\epsilon} \left(3 + 2 \log \frac{\mu_{\text{R}}^2}{m_H^2} \right) - \log^2 \left(\frac{\mu_{\text{R}}^2}{m_H^2} \right) + \pi^2 - 2 \right] |\mathcal{M}_{\text{tree}}|^2. \end{aligned} \quad (\text{A.4})$$

The remaining infrared divergences cancel with the integrated dipole subtraction terms. At the end, the finite result of the virtual correction reads

$$2\text{Re} [\mathcal{M}_{\text{loop+CT}} \cdot \mathcal{M}_{\text{tree}}^*] + \mathbf{I}(\epsilon) \times |\mathcal{M}_{\text{tree}}|^2 = \frac{\alpha_s C_F}{2\pi} \left(3 \log \frac{\mu_R^2}{m_H^2} + 8 \right) |\mathcal{M}_{\text{tree}}|^2, \quad (\text{A.5})$$

where the operator $\mathbf{I}(\epsilon)$ is the integrated dipole subtraction term [58, 59]. After performing the phase space integration, our result agrees with those in [73, 75, 80, 91].

B $H \rightarrow \gamma\gamma$ decay

The Higgs boson to a photon pair decay is a clean channel in discovering the Higgs boson. The QCD NLO corrections to this decay channel have been calculated in the heavy top quark limit [92–94] and with full quark mass dependence [95–99]. Higher-order results are also available [100–102]. Since the NLO QCD corrections do not contribute to the final result, as discussed around eq.(2.9), we consider the Higgs boson decay to a photon pair at LO. The relevant one-loop amplitude squared is given by [103]

$$|\mathcal{M}_{\text{one-loop}}(H \rightarrow \gamma\gamma)|^2 = \frac{G_F \alpha^2 m_H^4}{4\sqrt{2}\pi^2} \left| \sum_f N_c Q_f^2 A_f(\tau_f) + A_W(\tau_W) \right|^2, \quad (\text{B.1})$$

where N_c is the color factor, Q_f is the electric charge of the fermion f , and the variables $\tau_{f,W}$ are defined by

$$\tau_f = \frac{m_H^2}{4m_f^2}, \quad \tau_W = \frac{m_H^2}{4m_W^2}. \quad (\text{B.2})$$

The amplitude A_f and A_W can be expressed as

$$\begin{aligned} A_f(\tau) &= \frac{2[\tau + (\tau - 1)f(\tau)]}{\tau^2}, \\ A_W(\tau) &= -\frac{2\tau^2 + 3\tau + 3(2\tau - 1)f(\tau)}{\tau^2}, \end{aligned} \quad (\text{B.3})$$

where the function $f(\tau)$ is given by

$$f(\tau) = \begin{cases} \arcsin^2 \sqrt{\tau} & , \quad \tau \leq 1, \\ -\frac{1}{4} \left[\log \frac{1+\sqrt{1-\tau^{-1}}}{1-\sqrt{1-\tau^{-1}}} - i\pi \right]^2 & , \quad \tau > 1. \end{cases} \quad (\text{B.4})$$

References

- [1] **ATLAS** Collaboration, G. Aad et al., *Observation of a new particle in the search for the Standard Model Higgs boson with the ATLAS detector at the LHC*, *Phys. Lett. B* **716** (2012) 1–29, [[arXiv:1207.7214](#)].
- [2] **CMS** Collaboration, S. Chatrchyan et al., *Observation of a New Boson at a Mass of 125 GeV with the CMS Experiment at the LHC*, *Phys. Lett. B* **716** (2012) 30–61, [[arXiv:1207.7235](#)].

- [3] F. Englert and R. Brout, *Broken symmetry and the mass of gauge vector mesons*, *Phys. Rev. Lett.* **13** (Aug, 1964) 321–323.
- [4] P. Higgs, *Broken symmetries, massless particles and gauge fields*, *Physics Letters* **12** (1964), no. 2 132–133.
- [5] P. W. Higgs, *Broken symmetries and the masses of gauge bosons*, *Phys. Rev. Lett.* **13** (Oct, 1964) 508–509.
- [6] G. S. Guralnik, C. R. Hagen, and T. W. B. Kibble, *Global conservation laws and massless particles*, *Phys. Rev. Lett.* **13** (Nov, 1964) 585–587.
- [7] **CMS** Collaboration, A. M. Sirunyan et al., *A measurement of the Higgs boson mass in the diphoton decay channel*, *Phys. Lett. B* **805** (2020) 135425, [[arXiv:2002.06398](#)].
- [8] **ATLAS** Collaboration, *Measurement of the Higgs boson mass in the $H \rightarrow ZZ^* \rightarrow 4l$ decay channel using 139 fb^{-1} of $\sqrt{s} = 13 \text{ TeV}$ pp collisions recorded by the ATLAS detector at the LHC*, *Phys. Lett. B* **843** (2023) 137880.
- [9] **CMS** Collaboration, A. Tumasyan et al., *Measurement of the Higgs boson width and evidence of its off-shell contributions to ZZ production*, *Nature Phys.* **18** (2022), no. 11 1329–1334, [[arXiv:2202.06923](#)].
- [10] **ATLAS** Collaboration, G. Aad et al., *Study of the spin and parity of the Higgs boson in diboson decays with the ATLAS detector*, *Eur. Phys. J. C* **75** (2015), no. 10 476, [[arXiv:1506.05669](#)]. [Erratum: *Eur.Phys.J.C* 76, 152 (2016)].
- [11] **CMS** Collaboration, V. Khachatryan et al., *Constraints on the spin-parity and anomalous HVV couplings of the Higgs boson in proton collisions at 7 and 8 TeV*, *Phys. Rev. D* **92** (2015), no. 1 012004, [[arXiv:1411.3441](#)].
- [12] **ATLAS** Collaboration, *A detailed map of Higgs boson interactions by the ATLAS experiment ten years after the discovery*, *Nature* **607** (2022), no. 7917 52–59, [[arXiv:2207.00092](#)]. [Erratum: *Nature* 612, E24 (2022)].
- [13] **CMS** Collaboration, A. Tumasyan et al., *A portrait of the Higgs boson by the CMS experiment ten years after the discovery*, *Nature* **607** (2022), no. 7917 60–68, [[arXiv:2207.00043](#)].
- [14] G. Degrandi, S. Di Vita, J. Elias-Miro, J. R. Espinosa, G. F. Giudice, G. Isidori, and A. Strumia, *Higgs mass and vacuum stability in the Standard Model at NNLO*, *JHEP* **08** (2012) 098, [[arXiv:1205.6497](#)].
- [15] M. McCullough, *An Indirect Model-Dependent Probe of the Higgs Self-Coupling*, *Phys. Rev. D* **90** (2014), no. 1 015001, [[arXiv:1312.3322](#)]. [Erratum: *Phys.Rev.D* 92, 039903 (2015)].
- [16] M. Gorbahn and U. Haisch, *Indirect probes of the trilinear Higgs coupling: $gg \rightarrow h$ and $h \rightarrow \gamma\gamma$* , *JHEP* **10** (2016) 094, [[arXiv:1607.03773](#)].
- [17] G. Degrandi, P. P. Giardino, F. Maltoni, and D. Pagani, *Probing the Higgs self coupling via single Higgs production at the LHC*, *JHEP* **12** (2016) 080, [[arXiv:1607.04251](#)].
- [18] W. Bizon, M. Gorbahn, U. Haisch, and G. Zanderighi, *Constraints on the trilinear Higgs coupling from vector boson fusion and associated Higgs production at the LHC*, *JHEP* **07** (2017) 083, [[arXiv:1610.05771](#)].
- [19] **ATLAS** Collaboration, G. Aad et al., *Constraints on the Higgs boson self-coupling from*

- single- and double-Higgs production with the ATLAS detector using pp collisions at $s=13$ TeV*, *Phys. Lett. B* **843** (2023) 137745, [[arXiv:2211.01216](#)].
- [20] J. Gao, X.-M. Shen, G. Wang, L. L. Yang, and B. Zhou, *Probing the Higgs boson trilinear self-coupling through Higgs boson+jet production*, *Phys. Rev. D* **107** (2023), no. 11 115017, [[arXiv:2302.04160](#)].
- [21] S. Di Vita, C. Grojean, G. Panico, M. Riemann, and T. Vantalon, *A global view on the Higgs self-coupling*, *JHEP* **09** (2017) 069, [[arXiv:1704.01953](#)].
- [22] S. Dawson, S. Dittmaier, and M. Spira, *Neutral Higgs boson pair production at hadron colliders: QCD corrections*, *Phys. Rev. D* **58** (1998) 115012, [[hep-ph/9805244](#)].
- [23] D. de Florian and J. Mazzitelli, *Higgs Boson Pair Production at Next-to-Next-to-Leading Order in QCD*, *Phys. Rev. Lett.* **111** (2013) 201801, [[arXiv:1309.6594](#)].
- [24] D. de Florian, M. Grazzini, C. Hanga, S. Kallweit, J. M. Lindert, P. Maierhöfer, J. Mazzitelli, and D. Rathlev, *Differential Higgs Boson Pair Production at Next-to-Next-to-Leading Order in QCD*, *JHEP* **09** (2016) 151, [[arXiv:1606.09519](#)].
- [25] L.-B. Chen, H. T. Li, H.-S. Shao, and J. Wang, *Higgs boson pair production via gluon fusion at N^3 LO in QCD*, *Phys. Lett. B* **803** (2020) 135292, [[arXiv:1909.06808](#)].
- [26] L.-B. Chen, H. T. Li, H.-S. Shao, and J. Wang, *The gluon-fusion production of Higgs boson pair: N^3 LO QCD corrections and top-quark mass effects*, *JHEP* **03** (2020) 072, [[arXiv:1912.13001](#)].
- [27] S. Borowka, N. Greiner, G. Heinrich, S. P. Jones, M. Kerner, J. Schlenk, U. Schubert, and T. Zirke, *Higgs Boson Pair Production in Gluon Fusion at Next-to-Leading Order with Full Top-Quark Mass Dependence*, *Phys. Rev. Lett.* **117** (2016), no. 1 012001, [[arXiv:1604.06447](#)]. [Erratum: *Phys.Rev.Lett.* 117, 079901 (2016)].
- [28] S. Borowka, N. Greiner, G. Heinrich, S. P. Jones, M. Kerner, J. Schlenk, and T. Zirke, *Full top quark mass dependence in Higgs boson pair production at NLO*, *JHEP* **10** (2016) 107, [[arXiv:1608.04798](#)].
- [29] J. Baglio, F. Campanario, S. Glaus, M. Mühlleitner, M. Spira, and J. Streicher, *Gluon fusion into Higgs pairs at NLO QCD and the top mass scheme*, *Eur. Phys. J. C* **79** (2019), no. 6 459, [[arXiv:1811.05692](#)].
- [30] J. Baglio, F. Campanario, S. Glaus, M. Mühlleitner, J. Ronca, M. Spira, and J. Streicher, *Higgs-Pair Production via Gluon Fusion at Hadron Colliders: NLO QCD Corrections*, *JHEP* **04** (2020) 181, [[arXiv:2003.03227](#)].
- [31] M. Grazzini, G. Heinrich, S. Jones, S. Kallweit, M. Kerner, J. M. Lindert, and J. Mazzitelli, *Higgs boson pair production at NNLO with top quark mass effects*, *JHEP* **05** (2018) 059, [[arXiv:1803.02463](#)].
- [32] M. L. Czakon and M. Niggetiedt, *Exact quark-mass dependence of the Higgs-gluon form factor at three loops in QCD*, *JHEP* **05** (2020) 149, [[arXiv:2001.03008](#)].
- [33] J. Mazzitelli, *NNLO study of top-quark mass renormalization scheme uncertainties in Higgs boson production*, *JHEP* **09** (2022) 065, [[arXiv:2206.14667](#)].
- [34] J. Davies, K. Schönwald, and M. Steinhauser, *Towards $gg \rightarrow HH$ at next-to-next-to-leading order: Light-fermionic three-loop corrections*, *Phys. Lett. B* **845** (2023) 138146, [[arXiv:2307.04796](#)].

- [35] S. Borowka, C. Duhr, F. Maltoni, D. Pagani, A. Shivaaji, and X. Zhao, *Probing the scalar potential via double Higgs boson production at hadron colliders*, *JHEP* **04** (2019) 016, [[arXiv:1811.12366](#)].
- [36] M. Mühlleitner, J. Schlenk, and M. Spira, *Top-Yukawa-induced corrections to Higgs pair production*, *JHEP* **10** (2022) 185, [[arXiv:2207.02524](#)].
- [37] J. Davies, G. Mishima, K. Schönwald, M. Steinhauser, and H. Zhang, *Higgs boson contribution to the leading two-loop Yukawa corrections to $gg \rightarrow HH$* , *JHEP* **08** (2022) 259, [[arXiv:2207.02587](#)].
- [38] J. Davies, K. Schönwald, M. Steinhauser, and H. Zhang, *Next-to-leading order electroweak corrections to $gg \rightarrow HH$ and $gg \rightarrow gH$ in the large- m_t limit*, *JHEP* **10** (2023) 033, [[arXiv:2308.01355](#)].
- [39] H.-Y. Bi, L.-H. Huang, R.-J. Huang, Y.-Q. Ma, and H.-M. Yu, *Electroweak corrections to double Higgs production at the LHC*, [[arXiv:2311.16963](#)].
- [40] D. Y. Shao, C. S. Li, H. T. Li, and J. Wang, *Threshold resummation effects in Higgs boson pair production at the LHC*, *JHEP* **07** (2013) 169, [[arXiv:1301.1245](#)].
- [41] D. de Florian and J. Mazzitelli, *Higgs pair production at next-to-next-to-leading logarithmic accuracy at the LHC*, *JHEP* **09** (2015) 053, [[arXiv:1505.07122](#)].
- [42] A. H. Ajjath and H.-S. Shao, *N^3LO+N^3LL QCD improved Higgs pair cross sections*, *JHEP* **02** (2023) 067, [[arXiv:2209.03914](#)].
- [43] **ATLAS** Collaboration, *Measurement prospects of Higgs boson pair production in the $b\bar{b}\gamma\gamma$ final state with the ATLAS experiment at the HL-LHC*, *ATL-PHYS-PUB-2022-001* (2022).
- [44] **ATLAS** Collaboration, G. Aad et al., *Combination of searches for Higgs boson pairs in pp collisions at $\sqrt{s} = 13$ TeV with the ATLAS detector*, *Phys. Lett. B* **800** (2020) 135103, [[arXiv:1906.02025](#)].
- [45] **LHC Higgs Cross Section Working Group** Collaboration, D. de Florian et al., *Handbook of LHC Higgs Cross Sections: 4. Deciphering the Nature of the Higgs Sector*, [[arXiv:1610.07922](#)].
- [46] **HDECAY** Collaboration, A. Djouadi, J. Kalinowski, M. Muehlleitner, and M. Spira, *HDECAY: Twenty++ years after*, *Comput. Phys. Commun.* **238** (2019) 214–231, [[arXiv:1801.09506](#)].
- [47] A. Djouadi, J. Kalinowski, and M. Spira, *HDECAY: A Program for Higgs boson decays in the standard model and its supersymmetric extension*, *Comput. Phys. Commun.* **108** (1998) 56–74, [[hep-ph/9704448](#)].
- [48] S. Alioli, P. Nason, C. Oleari, and E. Re, *A general framework for implementing NLO calculations in shower Monte Carlo programs: the POWHEG BOX*, *JHEP* **06** (2010) 043, [[arXiv:1002.2581](#)].
- [49] **OpenLoops 2** Collaboration, F. Buccioni, J.-N. Lang, J. M. Lindert, P. Maierhöfer, S. Pozzorini, H. Zhang, and M. F. Zoller, *OpenLoops 2*, *Eur. Phys. J. C* **79** (2019), no. 10 866, [[arXiv:1907.13071](#)].
- [50] F. Buccioni, S. Pozzorini, and M. Zoller, *On-the-fly reduction of open loops*, *Eur. Phys. J. C* **78** (2018), no. 1 70, [[arXiv:1710.11452](#)].

- [51] A. Denner, S. Dittmaier, and L. Hofer, *Collier: a fortran-based Complex One-Loop Library in Extended Regularizations*, *Comput. Phys. Commun.* **212** (2017) 220–238, [[arXiv:1604.06792](#)].
- [52] A. van Hameren, *OneLOop: For the evaluation of one-loop scalar functions*, *Comput. Phys. Commun.* **182** (2011) 2427–2438, [[arXiv:1007.4716](#)].
- [53] J. Küblbeck, M. Böhm, and A. Denner, *Feyn arts — computer-algebraic generation of feynman graphs and amplitudes*, *Computer Physics Communications* **60** (1990), no. 2 165–180.
- [54] T. Hahn, *Generating Feynman diagrams and amplitudes with FeynArts 3*, *Comput. Phys. Commun.* **140** (2001) 418–431, [[hep-ph/0012260](#)].
- [55] R. Mertig, M. Böhm, and A. Denner, *Feyn calc - computer-algebraic calculation of feynman amplitudes*, *Computer Physics Communications* **64** (1991), no. 3 345–359.
- [56] V. Shtabovenko, R. Mertig, and F. Orellana, *New Developments in FeynCalc 9.0*, *Comput. Phys. Commun.* **207** (2016) 432–444, [[arXiv:1601.01167](#)].
- [57] V. Shtabovenko, R. Mertig, and F. Orellana, *FeynCalc 9.3: New features and improvements*, *Comput. Phys. Commun.* **256** (2020) 107478, [[arXiv:2001.04407](#)].
- [58] S. Catani and M. H. Seymour, *A General algorithm for calculating jet cross-sections in NLO QCD*, *Nucl. Phys. B* **485** (1997) 291–419, [[hep-ph/9605323](#)]. [Erratum: *Nucl.Phys.B* 510, 503–504 (1998)].
- [59] T. Gleisberg and F. Krauss, *Automating dipole subtraction for QCD NLO calculations*, *Eur. Phys. J. C* **53** (2008) 501–523, [[arXiv:0709.2881](#)].
- [60] S. Carrazza, R. K. Ellis, and G. Zanderighi, *QCDLoop: a comprehensive framework for one-loop scalar integrals*, *Comput. Phys. Commun.* **209** (2016) 134–143, [[arXiv:1605.03181](#)].
- [61] A. Buckley, J. Ferrando, S. Lloyd, K. Nordström, B. Page, M. Rüfenacht, M. Schönherr, and G. Watt, *LHAPDF6: parton density access in the LHC precision era*, *Eur. Phys. J. C* **75** (2015) 132, [[arXiv:1412.7420](#)].
- [62] M. Cacciari, G. P. Salam, and G. Soyez, *The anti- k_t jet clustering algorithm*, *JHEP* **04** (2008) 063, [[arXiv:0802.1189](#)].
- [63] M. Cacciari, G. P. Salam, and G. Soyez, *FastJet User Manual*, *Eur. Phys. J. C* **72** (2012) 1896, [[arXiv:1111.6097](#)].
- [64] **CMS** Collaboration, A. M. Sirunyan et al., *Search for nonresonant Higgs boson pair production in final states with two bottom quarks and two photons in proton-proton collisions at $\sqrt{s} = 13$ TeV*, *JHEP* **03** (2021) 257, [[arXiv:2011.12373](#)].
- [65] E. Braaten and J. P. Leveille, *Higgs Boson Decay and the Running Mass*, *Phys. Rev. D* **22** (1980) 715.
- [66] N. Sakai, *Perturbative QCD Corrections to the Hadronic Decay Width of the Higgs Boson*, *Phys. Rev. D* **22** (1980) 2220.
- [67] P. Janot, *First Order QED and QCD Radiative Corrections to Higgs Decay Into Massive Fermions*, *Phys. Lett. B* **223** (1989) 110–118.
- [68] M. Drees and K.-i. Hikasa, *NOTE ON QCD CORRECTIONS TO HADRONIC HIGGS DECAY*, *Phys. Lett. B* **240** (1990) 455. [Erratum: *Phys.Lett.B* 262, 497 (1991)].

- [69] J. Fleischer and F. Jegerlehner, *Radiative Corrections to Higgs Decays in the Extended Weinberg-Salam Model*, *Phys. Rev. D* **23** (1981) 2001–2026.
- [70] D. Y. Bardin, B. M. Vilensky, and P. K. Khristova, *Calculation of the Higgs boson decay width into fermion pairs*, *Sov. J. Nucl. Phys.* **53** (1991) 152–158.
- [71] A. Dabelstein and W. Hollik, *Electroweak corrections to the fermionic decay width of the standard Higgs boson*, *Z. Phys. C* **53** (1992) 507–516.
- [72] B. A. Kniehl, *Radiative corrections for $H \rightarrow f \text{ anti-}f (\gamma)$ in the standard model*, *Nucl. Phys. B* **376** (1992) 3–28.
- [73] S. G. Gorishnii, A. L. Kataev, S. A. Larin, and L. R. Surguladze, *Corrected Three Loop QCD Correction to the Correlator of the Quark Scalar Currents and γ (Tot) ($H^0 \rightarrow$ Hadrons)*, *Mod. Phys. Lett. A* **5** (1990) 2703–2712.
- [74] K. G. Chetyrkin, *Correlator of the quark scalar currents and Gamma(tot) ($H \rightarrow$ hadrons) at $O(\alpha_s^{**3})$ in pQCD*, *Phys. Lett. B* **390** (1997) 309–317, [[hep-ph/9608318](#)].
- [75] P. A. Baikov, K. G. Chetyrkin, and J. H. Kuhn, *Scalar correlator at $O(\alpha(s)**4)$, Higgs decay into b-quarks and bounds on the light quark masses*, *Phys. Rev. Lett.* **96** (2006) 012003, [[hep-ph/0511063](#)].
- [76] F. Herzog, B. Ruijl, T. Ueda, J. A. M. Vermaseren, and A. Vogt, *On Higgs decays to hadrons and the R-ratio at N^4LO* , *JHEP* **08** (2017) 113, [[arXiv:1707.01044](#)].
- [77] J. Davies, M. Steinhauser, and D. Wellmann, *Completing the hadronic Higgs boson decay at order α_s^4* , *Nucl. Phys. B* **920** (2017) 20–31, [[arXiv:1703.02988](#)].
- [78] X. Chen, P. Jakubčík, M. Marcoli, and G. Stagnitto, *The parton-level structure of Higgs decays to hadrons at N^3LO* , *JHEP* **06** (2023) 185, [[arXiv:2304.11180](#)].
- [79] C. Anastasiou, F. Herzog, and A. Lazopoulos, *The fully differential decay rate of a Higgs boson to bottom-quarks at NNLO in QCD*, *JHEP* **03** (2012) 035, [[arXiv:1110.2368](#)].
- [80] V. Del Duca, C. Duhr, G. Somogyi, F. Tramontano, and Z. Trócsányi, *Higgs boson decay into b-quarks at NNLO accuracy*, *JHEP* **04** (2015) 036, [[arXiv:1501.07226](#)].
- [81] R. Mondini, M. Schiavi, and C. Williams, *N^3LO predictions for the decay of the Higgs boson to bottom quarks*, *JHEP* **06** (2019) 079, [[arXiv:1904.08960](#)].
- [82] W. Bernreuther, L. Chen, and Z.-G. Si, *Differential decay rates of CP-even and CP-odd Higgs bosons to top and bottom quarks at NNLO QCD*, *JHEP* **07** (2018) 159, [[arXiv:1805.06658](#)].
- [83] A. Behring and W. Bizoń, *Higgs decay into massive b-quarks at NNLO QCD in the nested soft-collinear subtraction scheme*, *JHEP* **01** (2020) 189, [[arXiv:1911.11524](#)].
- [84] G. Somogyi and F. Tramontano, *Fully exclusive heavy quark-antiquark pair production from a colourless initial state at NNLO in QCD*, *JHEP* **11** (2020) 142, [[arXiv:2007.15015](#)].
- [85] K. G. Chetyrkin and A. Kwiatkowski, *Second order QCD corrections to scalar and pseudoscalar Higgs decays into massive bottom quarks*, *Nucl. Phys. B* **461** (1996) 3–18, [[hep-ph/9505358](#)].
- [86] R. Harlander and M. Steinhauser, *Higgs decay to top quarks at $O(\alpha_s^{**2})$* , *Phys. Rev. D* **56** (1997) 3980–3990, [[hep-ph/9704436](#)].
- [87] J. Wang, Y. Wang, and D.-J. Zhang, *Analytic decay width of the Higgs boson to massive bottom quarks at next-to-next-to-leading order in QCD*, [arXiv:2310.20514](#).

- [88] L. Mihaïla, B. Schmidt, and M. Steinhauser, $\Gamma(H \rightarrow b\bar{b})$ to order $\alpha\alpha_s$, *Phys. Lett. B* **751** (2015) 442–447, [[arXiv:1509.02294](#)].
- [89] Y. Hu, C. Sun, X.-M. Shen, and J. Gao, *Hadronic decays of Higgs boson at NNLO matched with parton shower*, *JHEP* **08** (2021) 122, [[arXiv:2101.08916](#)].
- [90] W. Bizoń, E. Re, and G. Zanderighi, *NNLOPS description of the $H \rightarrow b\bar{b}$ decay with $MinLO$* , *JHEP* **06** (2020) 006, [[arXiv:1912.09982](#)].
- [91] S. G. Gorishnii, A. L. Kataev, S. A. Larin, and L. R. Surguladze, *Scheme dependence of the next to next-to-leading QCD corrections to $\Gamma_{tot}(H \rightarrow \text{hadrons})$ and the spurious QCD infrared fixed point*, *Phys. Rev. D* **43** (1991) 1633–1640.
- [92] H.-Q. Zheng and D.-D. Wu, *First order QCD corrections to the decay of the Higgs boson into two photons*, *Phys. Rev. D* **42** (1990) 3760–3763.
- [93] A. Djouadi, M. Spira, J. J. van der Bij, and P. M. Zerwas, *QCD corrections to gamma gamma decays of Higgs particles in the intermediate mass range*, *Phys. Lett. B* **257** (1991) 187–190.
- [94] S. Dawson and R. P. Kauffman, *QCD corrections to $H \rightarrow \text{gamma gamma}$* , *Phys. Rev. D* **47** (1993) 1264–1267.
- [95] K. Melnikov and O. I. Yakovlev, *Higgs \rightarrow two photon decay: QCD radiative correction*, *Phys. Lett. B* **312** (1993) 179–183, [[hep-ph/9302281](#)].
- [96] A. Djouadi, M. Spira, and P. M. Zerwas, *Two photon decay widths of Higgs particles*, *Phys. Lett. B* **311** (1993) 255–260, [[hep-ph/9305335](#)].
- [97] J. Fleischer, O. V. Tarasov, and V. O. Tarasov, *Analytical result for the two loop QCD correction to the decay $H \rightarrow 2 \text{ gamma}$* , *Phys. Lett. B* **584** (2004) 294–297, [[hep-ph/0401090](#)].
- [98] R. Harlander and P. Kant, *Higgs production and decay: Analytic results at next-to-leading order QCD*, *JHEP* **12** (2005) 015, [[hep-ph/0509189](#)].
- [99] U. Aglietti, R. Bonciani, G. Degrossi, and A. Vicini, *Analytic Results for Virtual QCD Corrections to Higgs Production and Decay*, *JHEP* **01** (2007) 021, [[hep-ph/0611266](#)].
- [100] P. Maierhöfer and P. Marquard, *Complete three-loop QCD corrections to the decay $H \rightarrow \text{gamma gamma}$* , *Phys. Lett. B* **721** (2013) 131–135, [[arXiv:1212.6233](#)].
- [101] J. Davies and F. Herren, *Higgs boson decay into photons at four loops*, *Phys. Rev. D* **104** (2021), no. 5 053010, [[arXiv:2104.12780](#)].
- [102] M. Niggetiedt, *Exact quark-mass dependence of the Higgs-photon form factor at three loops in QCD*, *JHEP* **04** (2021) 196, [[arXiv:2009.10556](#)].
- [103] M. Spira, A. Djouadi, D. Graudenz, and P. M. Zerwas, *Higgs boson production at the LHC*, *Nucl. Phys. B* **453** (1995) 17–82, [[hep-ph/9504378](#)].